High-power vertical-cavity surface-emitting lasers bonded with efficient packaging

Changling Yan (晏长岭)[1*], Guoguang Lu (路国光)[2], and Li Qin (秦 莉)[2]

[1]*National Key Lab on High-Power Semiconductor Lasers, Changchun University of Science and Technology, Changchun 130022, China*

[2]*Changchun Institute of Optics, Fine Mechanics and Physics, Chinese Academy of Sciences, Changchun 130033, China*

[*]*E-mail: changling_yan@yahoo.com.cn*

Received November 12, 2009

High-power vertical-cavity surface-emitting lasers (VCSELs) are processed using a wet thermal-selective oxidation technique. The VCSEL chips are packaged by employing three different bonding methods of silver solder, In-Sn solder, and metalized diamond heat spreader. After packaging, optical output power, wavelength shift, and thermal resistance of the devices are measured and compared in an experiment. The device packaged with a metalized diamond heat spreader shows the best operation characteristics among the three methods. The 200-μm-diameter device bonded with a metalized diamond heat spreader produces a continuous wave optical output power of 0.51 W and a corresponding power density of 1.6 kW/cm^2 at room temperature. The thermal resistance is as low as 10 K/W. The accelerated aging test is also carried out at high temperature under constant current mode. The device operates for more than 1000 h at 70 °C, and the total degradation is only about 10%.

OCIS codes: 250.5960, 250.7260, 140.7260.

doi: 10.3788/COL20100806.0595.

Vertical-cavity surface-emitting lasers (VCSELs) are important semiconductor lasers with many advantages over conventional edge-emitting lasers, such as the circular beam profile, high packing density for two-dimensional arrays, and single longitudinal mode emission[1,2]. Low-power VCSELs have shown their suitability as information carriers in massive parallel optical interconnects, optical communications, and data storage applications[3−5]. Along with the rapid development of VCSELs with low output power, high-power VCSELs with large diameters or VCSEL arrays are also attracting enormous interest in many application areas such as free space communication, laser pumping, medicine, and material processing[6−8]. Normally, the air-bridge contacting and optocoupler design are widely studied in the fabrication and packaging of VCSEL devices for optical space communication[9]. For high-power semiconductor lasers, thermal effects are known to limit the optical output power and efficiency of the devices. Therefore, the device packaging technique should be given careful attention in high-power VCSELs. To obtain an efficient packaging method, different device packaging techniques should be investigated comparatively. To our knowledge, there are few studies focusing on the comparison of the characteristics of VCSELs fabricated with different packaging methods. Optical output power, wavelength shift with input electrical power, and thermal resistance are important indicators of the thermal properties of the devices. In this letter, a 200-μm-diameter VCSEL is fabricated using the oxidation technique. The performances of devices fabricated with three different packaging methods are compared through the experimental measurement of optical output power, wavelength shift, and thermal resistance.

The VCSEL epitaxial wafers in this study were all grown on n$^+$-GaAs (100) substrates by metal-organic vapor-phase epitaxy (MOVPE). The device structure consists of an active region containing three $In_{0.2}Ga_{0.8}As$ quantum wells (QWs) embedded in $GaAs_{0.92}P_{0.08}$ barriers sandwiched between n- and p-type $Al_{0.9}Ga_{0.1}As/Al_{0.12}Ga_{0.88}As$ distributed Bragg reflector (DBR) mirrors (Fig. 1). A 30-nm-thick $Al_{0.98}Ga_{0.02}As$ layer located between the active region and the p-type mirror was oxidized and converted to Al_xO_y in the fabrication process for current confinement. Light was emitted through the GaAs substrate. The details of the device structure can be found in Ref. [10].

Wet chemical etching was used to define circular mesas. The exposed $Al_{0.98}Ga_{0.02}As$ layer was oxidized in a water vapor atmosphere using nitrogen as a carrier gas at 420 °C to form a 200-μm-diameter aperture. After oxidation, the surface was passivated with Si_3N_4 passivation layer. The p-type Ti-Pt-Au contact on top of the mesa was evaporated and served as a metal pad for soldering. The GaAs substrate was thinned and polished down to about 130 μm, and an antireflection (AR) coating was deposited. Self-aligned lithography was used to define the n-type Au-Ge-Ni large-area electrical contact

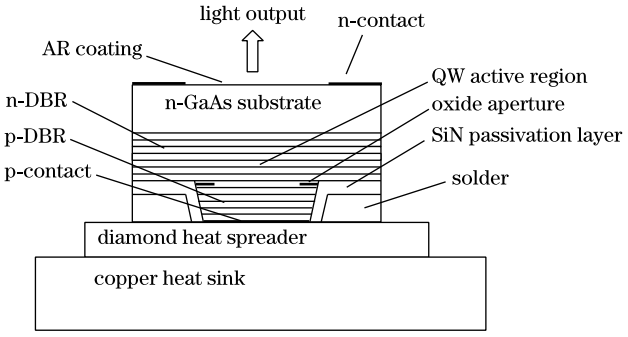

Fig. 1. Schematic diagram of the VCSEL structure.

surrounding the emission windows. The chip was annealed at 380 °C in a nitrogen environment condition, and a single device was separated by the cleaving technique. For the device packaging, the semiconductor laser chip was bonded at the junction down to a copper heat sink with three bonding methods: 1) the VCSEL was bonded to the copper heat sink with silver paste (Ag-In); 2) bonded to the copper heat sink with In-Sn solder; and 3) bonded to a metalized diamond heat spreader with In-Sn solder, then the whole chip was attached onto a copper heat sink with the Au-Sn solder for mechanical stability, as well as good thermal and electrical conductivity. After bonding, all of the devices were packed onto a TO-3 metal, so that we can package for measurement. The three packaging methods were studied by measuring optical output power, wavelength shift, and thermal resistance of the devices.

After packaging the VCSEL chips with three different bonding methods, optical output power, wavelength shift with input electrical power, and thermal resistance of the devices were measured and compared in an experiment. Figure 2 shows the continuous-wave (CW) power-current (P–I) curves of 200-μm-diameter VCSELs bonded with three different packaging methods. As shown in Fig. 2, the maximum room temperature CW output power from the device mounted to a metalized diamond heat spreader was the highest among the three packaging methods, exhibiting up to 0.51 W (corresponding to a power density of 1.6 kW/cm^2), and the slope efficiency is about 0.4 W/A. The maximum room temperature CW optical output power in the device mounted to a copper heat sink with silver paste was merely 0.1 W, with a slope efficiency of about 0.1 W/A. Low slope efficiency can result in more heat in the device, leading to a more evident lasing wavelength shift with the device internal heat. Conversion efficiency of the device bonded with a metalized diamond heat spreader was about 12%.

The devices operated at about 980-nm wavelength. Figure 3 shows the lasing wavelength shift as a function of the input electrical power for three different packaged devices. For the devices mounted to the copper heat sink with silver paste and In-Sn solder, the wavelength shifts were as large as 1.4 and 1.0 nm/W, respectively. The wavelength shift was about 0.5 nm/W for the device bonded with a metalized diamond heat spreader.

By measuring the thermal resistance of the device, the three packaging methods were also compared

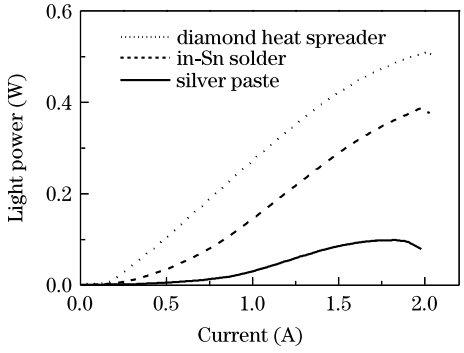

Fig. 2. Comparison of optical output characteristics of the devices bonded with silver paste, In-Sn solder, and metalized diamond heat spreader.

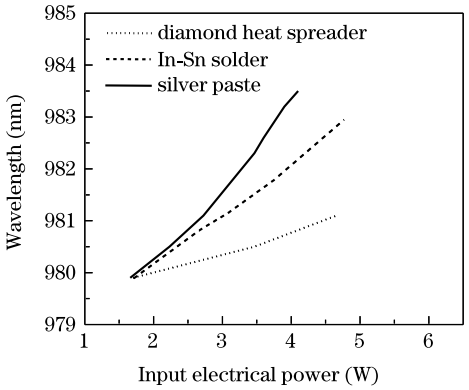

Fig. 3. Wavelength shift of the VCSEL spectrum as a function of input electrical power for the devices bonded with silver paste, In-Sn solder, and metalized diamond heat spreader.

in the experiment. Thermal resistance $R_{\rm th}$ of a device is generally defined as the temperature rise, ΔT, in the device with the change in power dissipation, ΔP:$R_{\rm th} = \Delta T/\Delta P$. Since the refractive index changes with temperature, the longitudinal-mode spectrum of a VCSEL will also change. By first measuring the wavelength change with temperature $\Delta\lambda/\Delta T$, and then measuring the wavelength change with the dissipated power $\Delta\lambda/\Delta P$, we can correlate temperature change to the change of dissipated electrical input power change and obtain the thermal resistance of the device[11].

During the measurements, the device temperature was controlled by a temperature controller through a thermoelectric cooler, which kept the bottom of the substrate at a constant temperature. The wavelength change of the VCSEL emission was measured with a spectrometer. The dissipated power was taken to be the input electrical power minus the output optical power. All the VCSELs used for bonding were made from the same VCSEL wafer and had a 200-μm-diameter aperture.

Table 1 summarizes the thermal resistance of the VCSELs with three bonding methods. The thermal resistance was 24 K/W for the device bonded with silver paste, 18 K/W for the device bonded with In-Sn solder, and 10 K/W for the device bonded with a metalized diamond heat spreader. The corresponding maximum optical output powers are also summarized in the table. From the experimental results, the device fabricated with the metalized diamond heat spreader packaging method showed the lowest thermal resistance and the highest output power compared with those of the two other methods.

VCSELs with 300-μm-diameter apertures were also fabricated using the oxidation technique. In the device

Table 1. Thermal Resistance and Maximum Output Power of VCSELs

Bonding Method	Silver Paste	In-Sn Solder	Metalized Diamond Heat Spreader
Thermal Resistance (K/W)	24	18	10
Maximum CW Output Power (W)	0.11	0.39	0.51

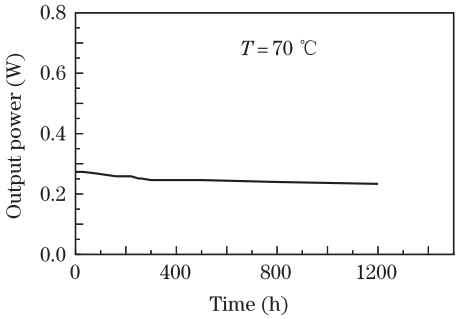

Fig. 4. Aging test of the VCSEL bonded with metalized diamond heat spreader under 1-A injection current at 70 °C.

packaging, the bonding with a metalized diamond heat spreader was selected for efficient heat extraction. The cleaved semiconductor chip was soldered at the junction down onto the metalized diamond heat spreader, then the whole chip was attached onto a copper heat sink.

The experimentally measured optical output power versus current characteristics of devices with 300-μm-diameter apertures was obtained. The maximum output power from the device was up to 1.0 W at room temperature and CW condition.

Reliability of a device is necessary for all applications; thus, an accelerated aging test of the 200-μm-diameter VCSEL bonded with a metalized diamond heat spreader was carried out. The devices operated at a high temperature of 70 °C under CW operation condition. Figure 4 shows the aging test from one device selected at random. The output power at the beginning of the test was 270 mW at 1-A constant current injection condition. The device ran for more than 1000 h, and the total degradation was about 10%. The device did not fail after the high temperature accelerated aging test.

In conclusion, by comparing the optical output power, wavelength shift with the input electrical power, and thermal resistance of the devices, the VCSEL chips bonded with three different packaging methods are investigated in an experiment. The 200-μm-diameter device bonded to a metalized diamond heat spreader produces a CW output power of 0.51 W, corresponding to the power density of 1.6 kW/cm^2, with low thermal resistance, indicating high-quality heat spreading. The accelerated aging test is also carried out at high temperature under constant current mode. The aging test result also shows the reliability of the device bonded with metalized diamond heat spreader. This packaging method is anticipated to meet the requirements of fabrication of other optoelectronic devices.

This work was supported by the National Natural Science Foundation of China under Grant Nos. 60676025 and 60306004.

References

1. R. S. Geels, S. W. Corzine, and L. A. Coldren, IEEE J. Quantum Electron. **27,** 1359 (1991).
2. T. Wang, X. Guo, B. Guan, and G. Shen, Chinese J. Lasers (in Chinese) **36,** 1057 (2009).
3. D. Wiedenmann, R. King, C. Jung, R. Jager, and R. Michalzik, IEEE J. Sel. Top. Quantum Electron. **5,** 503 (1999).
4. W. Wang, S. Zhang, X. Qian, and Y. Wang, Chin. Opt. Lett. **7,** 945 (2009).
5. Z. Wang, Y. Ning, Y. Zhang, J. Shi, T. Li, J. Cui, G. Liu, X. Zhang, L. Qin, Y. Sun, Y. Liu, and L. Wang, Chinese J. Lasers (in Chinese) **36,** 1963 (2009).
6. J. Diaz, H. J. Yi, M. Razeghi, and G. T. Burnham, Appl. Phys. Lett. **71,** 3042 (1997).
7. J. Wu, G. Iordache, H. D. Summers, and J. S. Roberts, Opt. Commun. **196,** 251 (2001).
8. E. S. Björlin, T. Kimura, Q. Chen, C. Wang, and J. E. Bowers, Electron. Lett. **40,** 121 (2004).
9. R. D. Briggs, M. G. Armendariz, K. M. Geib, K. D. Choquette, and D. K. Serkland, Proc. SPIE **3627,** 40 (1999).
10. C. Yan, Y. Ning, L. Qin, Y. Liu, L. Zhao, Q. Wang, Z. Jin, Y. Sun, G. Tao, G. Chu, C. Wang, L. Wang, and H. Jiang, Electron. Lett. **40,** 872 (2004).
11. M. H. MacDougal, J. Geske, C.-K. Lin, A. E. Bond, and P. D. Dapkus, IEEE Photon. Technol. Lett. **10,** 15 (1998).